JASR 6703
TYPED/ 3/4/04

ARTICLE IN PRESS

No. of pages: 8
DTD 4.3.1 / SPS-N

ELSEVIER

Available online at www.sciencedirect.com

SCIENCE @ DIRECT®

Advances in Space Research xxx (2004) xxx–xxx

ADVANCES IN SPACE RESEARCH
(a COSPAR publication)

www.elsevier.com/locate/asr

An improved Green's function for ion beam transport

J. Tweed [a,*], J.W. Wilson [b], R.K. Tripathi [b]

[a] *Department of Mathematics and Statistics, Old Dominion University, Hampton Blvd, Norfolk, VA 23529-0077, USA*
[b] *NASA Langley Research Center, Hampton, VA 23681-2199, USA*

Received 19 October 2002; received in revised form 16 November 2003; accepted 23 November 2003

Abstract

Ion beam transport theory allows testing of material transmission properties in the laboratory environment generated by particle accelerators. This is a necessary step in materials development and evaluation for space use. The approximations used in solving the Boltzmann transport equation for the space setting are often not sufficient for laboratory work and those issues are the main emphasis of the present work. In consequence, an analytic solution of the linear Boltzmann equation is pursued in the form of a Green's function allowing flexibility in application to a broad range of boundary value problems. It has been established that simple solutions can be found for the high charge and energy (HZE) by ignoring nuclear energy downshifts and dispersion. Such solutions were found to be supported by experimental evidence with HZE ion beams when multiple scattering was added. Lacking from the prior solutions were range and energy straggling and energy downshift with dispersion associated with nuclear events. Recently, we have found global solutions including these effects providing a broader class of HZE ion solutions.

Keywords: Radiation risk; Boltzman transport equation; Ion beam transport; An improved Green's function

1. Introduction

In space radiation transport, the energy lost through atomic collisions is treated as averaged processes over the many events which occur over even relatively small dimensions of most materials and is referred to as the continuous slowing down approximation. It is reasoned that the few percent energy fluctuation in energy loss has little meaning for ions of broad energy spectra and especially in comparison to the many nuclear events for which uncertainties are still relatively large. In contrast, the laboratory testing of potential shielding materials uses nearly monoenergetic ion beams in which the interpretation of the interaction with shield materials requires a detailed description of the interaction process for comparison to detector responses (Schimmerling et al., 1986). The development of a Green's function approach to ion transport facilitates the modeling of laboratory radiation environments and allows for the direct testing of transport approximations of material transmission properties. For a number of years, this approach has played a fundamental role in transport calculations for high-charge high-energy (HZE) ions and has been used to great effect by radiation investigators at the NASA, Langley Research Center. These earlier works have not, however, taken into account such effects as straggling or of the energy downshift with dispersion which occur whenever a nuclear event takes place. In addition to the validation of physical processes, a theoretical model of the role of straggling is essential to understanding of the radiobiology of ion beams as required in evaluation of astronaut risks which must be minimized at least to within some regulated level (Shinn et al., 1999). The present development is in the context of an asymptotic expansion of the 3D Boltzmann equation, for which, the lowest order term is along the forward ray. Additional asymptotic terms are discussed in an earlier work (Wilson et al., 1991) and a related paper (Wilson et al., 2002a).

* Corresponding author. Tel.: +1-757-683-3909; fax: +1-757-683-3885.
E-mail address: jtweed@odu.edu (J. Tweed).

0273-1177/$30 © 2004 COSPAR. Published by Elsevier Ltd. All rights reserved.
doi:10.1016/j.asr.2003.11.021

2. The Boltzmann equation

The specification of the interior environment of a spacecraft and evaluation of the effects on the astronaut is at the heart of the space radiation protection problem. For some time investigators at The NASA Langley Research Center have been developing techniques to address this problem and an in-depth presentation of their work is given by Wilson et al. (1991) although considerable progress has been made since that publication (Cucinotta et al., 1998). The relevant transport equation is the linear Boltzmann equation. The lowest order asymptotic term is the straightahead approximation. With the target secondary fragments neglected, Wilson et al. (1991), this equation takes the following form:

$$\partial_z \phi_j(Z,E) = \sum_{k \geqslant j} \int \sigma_{jk}(E,E')\phi_k(z,E')\,\mathrm{d}E' - \sigma_j(E)\phi_j(Z,E), \quad z \geqslant Z', \tag{1}$$

where $\phi_j(z,E)$ is the flux of ions of type j moving along the z-axis at energy E in units of MeV/amu and $\sigma_j(E)$ and $\sigma_{jk}(E,E')$ are the media macroscopic cross-sections. The $\sigma_{jk}(E,E')$ represent all those processes by which type k particles moving in the z-direction with energy E' produce a type j particle with energy E moving in the same direction. Note that there may be several reactions which produce a particular product, and the appropriate cross-sections for Eq. (1) are the inclusive ones. The total cross-section $\sigma_j(E)$ with the medium for each particle type of energy E may be expanded as

$$\sigma_j(E) = \sigma_j^{\mathrm{at}}(E) + \sigma_j^{\mathrm{el}}(E) + \sigma_j^{\mathrm{r}}(E), \tag{2}$$

where the first term refers to collision with atomic electrons, the second term is for elastic nuclear scattering, and the third term describes nuclear reactions. The corresponding differential cross-section is given as

$$\sigma_{jk}(E,E') = \sum_n \sigma_{j,n}^{\mathrm{at}}(E')\delta_{jk}\delta(E - E' + \varepsilon_n) + \sigma_j^{\mathrm{el}}(E')\delta_{jk}\delta(E - E') + \frac{\sigma_{jk}^{\mathrm{r}}(E')}{\sqrt{(2\pi)}\varepsilon_{jk}} \times \exp\left[-\frac{(E + \lambda_{jk} - E')^2}{2\varepsilon_{jk}^2}\right], \tag{3}$$

where ε_n are the atomic/molecular excitation energy levels and where the collision energy downshift λ_{jk} and corresponding energy width ε_{jk} are approximated from the known momentum distributions observed in heavy ion reactions and represented by a gaussian model. Many atomic collisions ($\sim 10^6$) occur in a centimeter of ordinary matter, whereas $\sim 10^3$ nuclear coulomb elastic collisions occur per centimeter, while nuclear reactions are separated by a fraction to many centimeters depending on energy and particle type. This ordering allows flexibility in expanding solutions to the Boltzmann equation as a sequence of physical perturbative approximations.

We require to solve Eq. (1) subject to a boundary condition of the type $\phi_j(z',E) = F_j(E)$. In the case of a unit source at the boundary, $F_j(E)$ takes the special form

$$F_j(E) = \delta_{jk}\delta(E - E'), \tag{4}$$

and the corresponding solution, which is called the Green's function, is denoted by the symbol $G_{jk}(z,z',E,E')$. Once the Green's function is known the solution for an arbitrary boundary condition $F_j(E)$ is then given by

$$\phi_j(z,E) = \sum_k \int G_{jk}(z,z',E,E'')F_k(E'')\,\mathrm{d}E''. \tag{5}$$

In the case of an accelerator beam, the boundary condition consists of a narrow gaussian function in energy and is incorporated by addition to the straggling width on leaving the boundary. In the case of space radiations, the boundary condition is represented as a broad function of energy and direction for each ion type and is handled by ordinary numerical procedures. It should also be noted that Eq. (5) provides a basis for multiple layers of materials by matching the solution at the boundary interface.

3. Solution methods

We rewrite Eq. (1) in operator notation by defining a vector array field function as

$$\Phi = [\phi_j(z,E)], \tag{6}$$

the drift operator

$$D = [\partial_z], \tag{7}$$

the interaction operator

$$I = \Xi - \sigma = \left[\int \sigma_{jk}(E,E')\,\mathrm{d}E'\right] - [\sigma_j(E)], \tag{8}$$

with the understanding that I has three parts associated with atomic, elastic, and reactive processes as given in Eqs. (2) and (3). Eq. (1) is then rewritten as

$$D \cdot \Phi = I \cdot \Phi = [I^{\mathrm{at}} + I^{\mathrm{el}} + I^{\mathrm{r}}] \cdot \Phi, \tag{9}$$

and one must look for solutions. In what follows, we will recall the solution of the atomic interactions by Payne (1969) and implemented by Wilson et al. (2002b). Effectively, we look at

$$D \cdot \Phi = I^{\mathrm{at}} \cdot \Phi, \tag{10}$$

which must then be coupled to the remaining terms in Eq. (9). For analysis, it will be advantageous to make the following separations:

$$[D - I^{\mathrm{at}} - I^{\mathrm{el}} + \sigma^{\mathrm{r}}] \cdot \Phi = \left[\int \sigma_{jk}^{\mathrm{r}}(E,E')\,\mathrm{d}E'\right] \cdot \Phi = \Xi^{\mathrm{r}} \cdot \Phi. \tag{11}$$

3.1. Atomic processes

The lowest order approximation to the Boltzmann equation is given in terms of the atomic collision processes as

$$D \cdot \Phi = I^{\mathrm{at}} \cdot \Phi, \tag{12}$$

with the boundary condition

$$\Phi_{\mathrm{B}} = [\phi_j(z', E)] = [\delta_{jk}\delta(E - E')]. \tag{13}$$

The solution, which incorporates energy straggling, takes the form

$$\phi_j(z,E) = \frac{\delta_{jk}}{\sqrt{2\pi}s'_k(z-z')} \exp\left[-\frac{(E - \langle E'_k(z-z')\rangle)^2}{2s'_k(z-z')^2} \right], \tag{14}$$

where

$$\langle E'_k(z-z')\rangle = R_k^{-1}[R_k(E') - (z - z')], \tag{15}$$

where $R_k(E)$ is the usual range-energy relation and $s'_k(z-z')$ is the rms deviation for incident k-type particles of energy E' after a distance of penetration $z - z'$ (Wilson et al., 2002b).

3.2. Elastic scattering processes

The addition of elastic scattering processes is given by

$$D \cdot \Phi = [I^{\mathrm{at}} + I^{\mathrm{el}}] \cdot \Phi. \tag{16}$$

Since we have approximated the elastic scattering distribution by

$$\sigma^{\mathrm{el}}_{jk}(E,E') = \sigma^{\mathrm{el}}_j(E')\delta_{jk}\delta(E - E'), \tag{17}$$

we find that

$$[I^{\mathrm{el}}] \cdot \Phi \approx [0], \tag{18}$$

and thus

$$D \cdot \Phi \approx [I^{\mathrm{at}}] \cdot \Phi. \tag{19}$$

Elastic scattering does not appear in the first asymptotic term evaluated herein. The first correction will contain elastic scattering as a dominant term for the propagation of the surviving primary beam ions and in some boundary problems involving collimators elastic scattering will play a role for higher order terms. The elastic scattering propagator is a focus of current research and will couple with the present formalism. In the past, this coupling was in terms of acceptance functions and provided good agreement with neon ion beams (Shavers et al., 1993).

3.3. Nuclear reactive processes

Following the above analysis, we are left with

$$[D - I^{\mathrm{at}} + \sigma^{\mathrm{r}}] \cdot \Phi = \left[\int \sigma^{\mathrm{r}}_{jk}(E,E')\,\mathrm{d}E' \right] \cdot \Phi = \Xi^{\mathrm{r}} \cdot \Phi. \tag{20}$$

In the present work, we approximate the fragment energy distribution by

$$\sigma^{\mathrm{r}}_{jk}(E,E') = \frac{\sigma^{\mathrm{r}}_{jk}(E')}{\sqrt{2\pi}\varepsilon_{jk}} \exp\left[-\frac{(E + \lambda_{jk} - E')^2}{2\varepsilon^2_{jk}} \right], \tag{21}$$

where λ_{jk} is the collision energy downshift (MeV/amu) and ε_{jk} is the interaction energy width (MeV/amu). λ_{jk} is related to the momentum downshift (MeV/c)

$$p_{\mathrm{s}} = 3.64\left(9 + \frac{A_j}{A_k}\right)\sqrt{\frac{9}{A_k^{1/3}} - \frac{5}{A_k^{2/3}}} - 28, \tag{22}$$

via the equation

$$\lambda_{jk} = \frac{p(E)p_{\mathrm{s}}}{A_j(m+E)}, \tag{23}$$

where A_k is the projectile mass (amu), A_j is the fragment mass (amu), E is the fragment energy (MeV/amu), m is the energy equivalent of a proton mass and

$$p(E) = \sqrt{E^2 + 2mE}, \tag{24}$$

is the fragment momentum (MeV/amu/c). The interaction energy width is similarly related to the momentum width σ_{F} (MeV/c) through the equation

$$\varepsilon_{jk} = \frac{p(E)\sigma_{\mathrm{F}}}{A_j(m+E)}, \tag{25}$$

where σ_{F} is given as (Tripathi et al., 1994)

$$\sigma_{\mathrm{F}} = \sqrt{\frac{1}{2}m\left(\frac{45}{A_k^{1/3}} - \frac{25}{A_k^{2/3}}\right)\left(\frac{A_j(A_k - A_j)}{A_k - 1}\right)}. \tag{26}$$

We start with the solution of the equation

$$[D - I^{\mathrm{at}} + \sigma^{\mathrm{r}}] \cdot G^0 = [0], \tag{27}$$

for a unit source at the boundary. Note that G^0 is diagonal and takes the form

$$G^0_{jk}(z,z',E,E') = \frac{P_k(E')}{P_j(E)} \frac{\delta_{jk}}{\sqrt{2\pi}s'_k(z-z')} \times \exp\left[-\frac{(E - \langle E'_k(z-z')\rangle)^2}{2s'_k(z-z')^2} \right], \tag{28}$$

where the nuclear attenuation is described by the function

$$P_k(E) = \exp\left[-\int_0^E \frac{\sigma^{\mathrm{r}}_k(E')}{S_k(E')}\,\mathrm{d}E' \right], \tag{29}$$

and $S_k(E)$ is the change in E per unit path length per nucleon. Eq. (28) and the reactive integral operator are all that is required to develop the solution under the straightahead approximation. The lateral spread of the beam is beyond the scope of the present development. So far all of the operators have had only diagonal elements. Off-diagonal elements enter through the reactive regeneration terms σ^{r}_{jk} which appear on the right side of Eq. (20). The challenge is to further develop the solution of Eq. (20) and this will be accomplished as follows. The integral form of Eq. (20) can be written as

$$\begin{aligned}\Phi &= [D - I^{at} + \sigma^{r}]^{-1}\cdot\Phi_B + \int_{z'}^{z}[D - I^{at} + \sigma^{r}]^{-1}\cdot\Xi^{r}\cdot\Phi\,\mathrm{d}z_1\\ &= G^0\cdot\Phi_B + Q\cdot G^0\cdot\Xi^{r}\cdot\Phi,\end{aligned} \tag{30}$$

where Φ_B is the appropriate boundary condition. Eq. (30) is a Volterra integral equation and is easily solved in a Neumann series as

$$\begin{aligned}\Phi &= [G^0 + Q\cdot G^0\cdot\Xi^{r}\cdot G^0 + Q\cdot G^0\cdot\Xi^{r}\cdot Q\cdot G^0\cdot\Xi^{r}\\ &\quad\cdot Q\cdot G^0 + \cdots]\cdot\Phi_B\\ &= [G^0 + G^1 + G^2 + \cdots]\cdot\Phi_B,\end{aligned} \tag{31}$$

with the elements of the leading term given as Eq. (28). The above formalism lends the following interpretation of the solution. The operator G^0 propagates the particles with attenuation processes. The first term $G^0\cdot\Phi_B$ propagates the ions at the boundary to the interior. $\Xi^{r}\cdot G^0\cdot\Phi_B$ is the production density of first generation secondaries at depth z_1. These are propagated to the interior by $G^0\cdot\Xi^{r}\cdot G^0\cdot\Phi_B$. Lastly, $G^1\cdot\Phi_B = Q\cdot G^0\cdot\Xi^{r}\cdot G^0\cdot\Phi_B$ represents the sum of all the first generation secondaries being propagated from the interval $[z', z]$ and so on. We have already identified the propagator G^0. We now need to identify the remaining terms in the Neumann series and we begin noting that these are related via the recurrence formula

$$G^{n+1} = [Q\cdot G^0\cdot\Xi^{r}]\cdot G^{n},\quad n\geqslant 0. \tag{32}$$

3.4. First collision term

The second term in Eq. (31) is the *first collision term*

$$\begin{aligned}G^1_{jk}(z,z',E,E') &= [Q\cdot G^0\cdot\Xi^{r}\cdot G^0]_{jk}(z,z',E,E')\\ &= \int_{z'}^{z}\int G^0_{jj}(z,z_1,E,E_2)\\ &\quad\times\left\{\int\sigma^{r}_{jk}(E_2,E_1)\right.\\ &\quad\left.\times G^0_{kk}(z,z',E,E')\mathrm{d}E_1\right\}\mathrm{d}E_2\,\mathrm{d}z_1.\end{aligned} \tag{33}$$

The physical interpretation is that $\Xi^{r}\cdot G^0$ is the volume source of ions from collisions at z_1 of a unit ion source at z' of energy E' The ions present at z with energy E are the result of propagation from the all the ions through out the volume. The first task is to evaluate the volume source term

$$\begin{aligned}&[\Xi^{r}\cdot G^0]_{jk}(z_1,z',E_2,E')\\ &= \int\frac{\sigma^{r}_{jk}(E_1)}{\sqrt{(2\pi)}\varepsilon_{jk}}\exp\left[-\frac{(E_2+\lambda_{jk}-E_1)^2}{2\varepsilon^2_{jk}}\right]\\ &\quad\times\frac{P_k(E')}{P_k(E_1)}\cdot\frac{1}{\sqrt{2\pi}s'_k(z-z')}\exp\left[-\frac{(E_1-\langle E'_k(z-z')\rangle)^2}{2s'_k(z-z')^2}\right]\mathrm{d}E_1.\end{aligned} \tag{34}$$

Note that a sharp maximum occurs at $E_1 = \langle E'_k(z-z')\rangle$, $E_2 = E_1 - \lambda_{jk}$ and the cross-sections and attenuation functions are slowly varying functions of energy so that Eq. (34) can be accurately approximated as

$$\begin{aligned}&[\Xi^{r}\cdot G^0]_{jk}(z_1,z',E_2,E')\\ &= \frac{P_k(E')}{P_k(\langle E'_k(z_1-z')\rangle)}\sigma^{r}_{jk}(\langle E'_k(z_1-z')\rangle)\\ &\quad\times\frac{1}{\sqrt{2\pi[s'_k(z-z')^2+\varepsilon^2_{jk}]}}\\ &\quad\times\exp\left\{-\frac{(E_2+\lambda_{jk}-\langle E'_k(z-z')\rangle)^2}{2[s'_k(z-z')^2+\varepsilon^2_{jk}]}\right\}.\end{aligned} \tag{35}$$

The next step is to construct the term

$$\begin{aligned}&[G^0\cdot\Xi^{r}\cdot G^0]_{jk}(z,z_1,z',E,E')\\ &= \int\frac{P_j(E_2)}{P_j(E)\sqrt{2\pi}s''_j(z-z_1)}\exp\left\{-\frac{[E-\langle E''_j(z-z_1)\rangle]^2}{2s''_j(z-z_1)^2}\right\}\\ &\quad\times\frac{P_k(E')}{P_k(\langle E'_k(z_1-z')\rangle)}\frac{\sigma^{r}_{jk}(\langle E'_k(z_1-z')\rangle)}{\sqrt{2\pi[s'_k(z-z')^2+\varepsilon^2_{jk}]}}\\ &\quad\times\exp\left\{-\frac{(E_2+\lambda_{jk}-\langle E'_k(z-z')\rangle)^2}{2[s'_k(z-z')^2+\varepsilon^2_{jk}]}\right\}\mathrm{d}E_2,\end{aligned} \tag{36}$$

where $\langle E''_j(z-z_1)\rangle = R_j^{-1}[R_j(E_2)-(z-z_1)]$ and $s''_j(z-z_1)$ is the corresponding spread. The integral has a sharp maximum at $E_2 = \langle E'_k(z_1-z')\rangle\lambda_{jk} \equiv \langle E_2\rangle$, $E = \langle E''_j(z-z_1)\rangle \equiv \langle E_j(z)\rangle$, where the cross-sections,attenuation functions, and straggling widths are evaluated. We expand $\langle E''_j(z-z_1)\rangle$ about the maximal value of E_2 to obtain

$$z\langle E''_j(z-z_1)\rangle \approx \langle E_j(z)\rangle + r_{jk}[E_2 - (\langle E'_k(z_1-z')\rangle - \lambda_{jk})], \tag{37}$$

where

$$r_{jk} = [\partial_{E_2}\langle E''_j(z-z_1)\rangle]_{\langle E_2\rangle} = \frac{S_j[\langle E_j(z)\rangle]}{S_j[\langle E_2\rangle]}. \tag{38}$$

Substituting Eq. (37) into the integral (36), making the change of variables $x = r_{jk}[E_2 - (\langle E'_k(z_1-z')\rangle - \lambda_{jk})]$ and integrating with respect to x results in

$$[G^0 \cdot \Xi^r \cdot G^0]_{jk}(z,z_1,z',E,E') = \frac{P_j(\langle E'_k(z_1-z')\rangle - \lambda_{jk})P_k(E')}{P_j(E)P_k(\langle E'_k(z_1-z')\rangle)} \cdot \frac{\sigma^r_{jk}(\langle\langle E'_k(z_1-z')\rangle\rangle)}{\sqrt{2\pi s^2_{jk}(z_1)}} \exp\left\{-\frac{[E-f_j(z_1)]}{2s^2_{jk}(z_1)}\right\}, \quad (39)$$

where

$$f_j(z_1) = R_j^{-1}\{R_j[\langle E'_k(z_1-z')\rangle - \lambda_{jk}] - (z-z_1)\} \quad (40)$$

and

$$s_{jk}(z_1) = \sqrt{r^2_{jk}\left[s'_k(z_1-z')^2 + \varepsilon^2_{jk}\right] + s''_j(z-z_1)^2}. \quad (41)$$

Lastly, we need to evaluate the integral

$$G^1_{jk}(z,z',E,E') = [Q \cdot G^0 \cdot \Xi^r \cdot G^0]_{jk}(z,z_1,z',E,E') = \int_{z'}^{z} [G^0 \cdot \Xi^r \cdot G^0]_{jk}(z,z_1,z',E,E')\,dz_1. \quad (42)$$

For a given set of parameters z, E, z', E', there is a value z_m of z_1 at which the integrand of (42) achieves a maximum and at which slowly varying factors entering the integrand may be computed. Thus

$$G^1_{jk}(z,z',E,E') \approx \frac{P_j(\langle E'_k(z_m-z')\rangle - \lambda_{jk})P_k(E')}{P_j(E)P_k(\langle E'_k(z_m-z')\rangle)} \times \frac{\sigma^r_{jk}(\langle\langle E'_k(z_m-z')\rangle\rangle)}{\sqrt{2\pi s^2_{jk}(z_m)}} \times \int_{z'}^{z} \exp\left\{-\frac{[E-f_j(z_1)]^2}{2s^2_{jk}(z_m)}\right\}dz_1. \quad (43)$$

The point z_m at which the integrand of (43) achieves its maximum is given by the equation

$$f_j(z_m) = E, \quad (44)$$

and is easily obtained by the routine root finding techniques. It is not difficult to show that

$$f'_j(z_m) = \left\{1 - \frac{S_k[\langle E'_k(z_m-z')\rangle]}{S_j[\langle E'_k(z_m-z')\rangle - \lambda_{jk}]}\right\}S_j[f_j(z_m)]. \quad (45)$$

Therefore, in (43) we may use the substitution $x = [E - f_j(z_1)]/[\sqrt{2}s_{jk}(z_m)]$ and then integrate to get

$$G^1_{jk}(z,z',E,E') = \frac{P_j[\langle E'_k(z_m-z')\rangle - \lambda_{jk}]P_k[E']}{P_j(E)P_k(\langle E'_k(z_m-z')\rangle)} \times \frac{\sigma^r_{jk}(\langle\langle E'_k(z_m-z')\rangle\rangle)}{2f'_j(z_m)} \times \left\{\mathrm{erf}\left[\frac{E-f_j(z')}{\sqrt{2}s_{jk}(z_m)}\right] - \mathrm{erf}\left[\frac{E-f_j(z)}{\sqrt{2}s_{jk}(z_m)}\right]\right\}, \quad (46)$$

where $s_{jk}(z_1)$ is given by (41).

3.5. Second collision term

The third term in Eq. (31) is the *second collision term*

$$G^2_{jk}(z,z',E,E') = [Q \cdot G^0 \cdot \Xi^r \cdot G^1]_{jk}(z,z',E,E') = \int_{z'}^{z}\int G^0_{jj}(z,z_1,E,E_2 1) \times \left\{\sum_{p>j}\int \sigma^r_{jp}(E_2,E_1) \times G^1_{pk}(z_1,z',E_1,E')\,dE_1\right\}dE_2\,dz_1. \quad (47)$$

On making approximations similar to those used in the previous section, Eq. (47) is reduced to the form

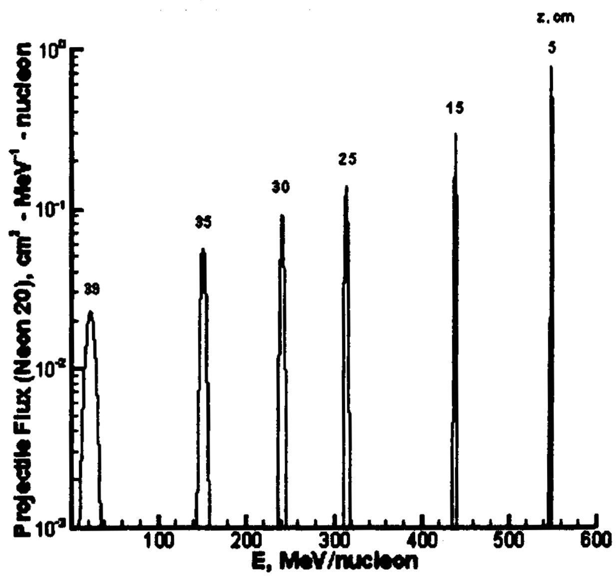

Fig. 1. Primary ion flux at various depths for Ne(20,10) incident on aluminum at 600 MeV/amu.

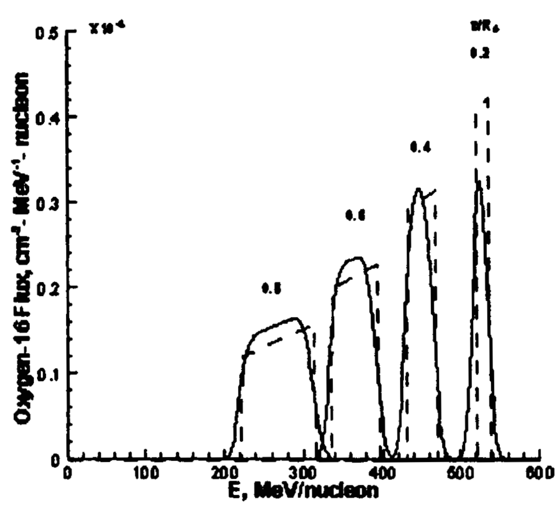

Fig. 2. First generation O(16,8) fragment flux at various depths compared with previous results (broken curve).

$$G_{jk}^{2}(z,z',E,E') = \sum_{p>j} \int_{z'}^{z} \frac{P_j[\overline{E}_j]S_j[\overline{E}_j]}{P_j[E]S_j[E]} \sigma_{jp}^{r}(\overline{E}_j + \lambda_{jp}) \times G_{pk}^{1}(z_1, z', \overline{E}_j + \lambda_{jp}, E')\mathrm{d}z_1, \quad (48)$$

where

$$\overline{E}_j = R_j^{-1}[R_j(E) + z - z_1], \quad (49)$$

and is then evaluated by numerical quadrature.

4. Results

Shown in this section are some results for the $_{8}O^{16}$ fragments which are produced when a beam of $_{10}Ne^{20}$ ions strikes an aluminum target at 600 MeV/amu. The results presented are similar to those obtained for other ions.

Fig. 1 shows the flux of the primary beam at various depths and exhibits the effects of energy straggling. In contrast to earlier works in which the primary beam appears as a propagating delta function, we see here that the primary beam attenuates and widens with depth. Note that the greatest depths in Fig. 1 are beyond the 85% range where straggling propagators of the past have failed.

Figs. 2 and 3 show the flux of the first and second generation of $_{8}O^{16}$ ions produced, respectively, in comparison with the corresponding flux (broken curves) obtained from an earlier approximate code using a non-

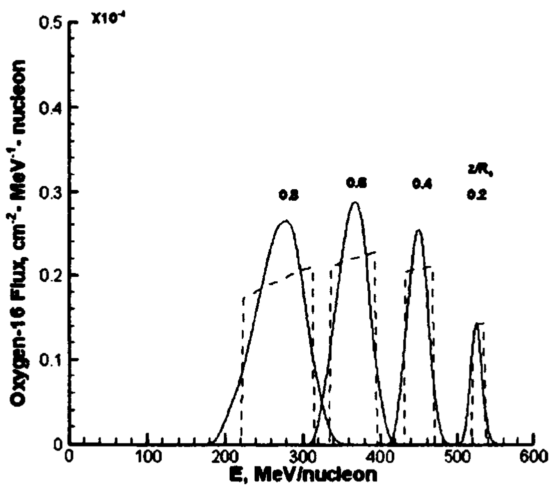

Fig. 3. Second generation O(16,8) fragment flux at various depths compared with previous results (broken curve).

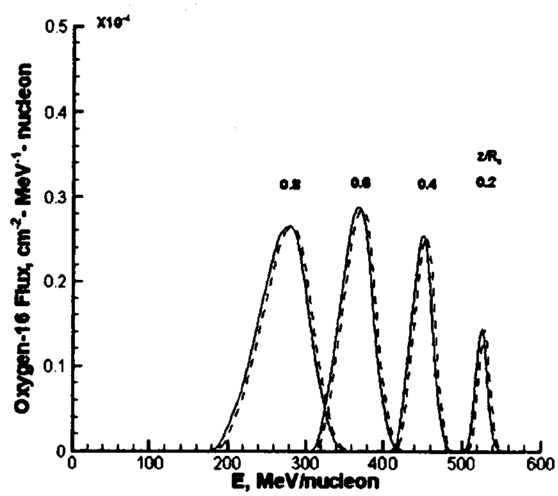

Fig. 5. Second generation O(16,8) fragment flux at various depths compared with the same flux for the case in which the collision energy downshift is zero (broken curve).

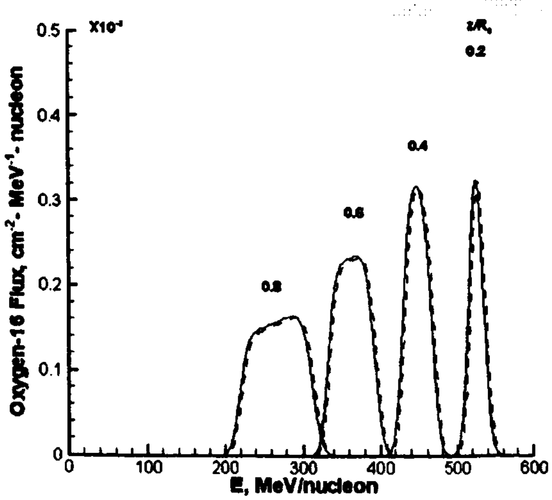

Fig. 4. First generation O(16,8) fragment flux at various depths compared with the same flux for the case in which the collision energy downshift is zero (broken curve).

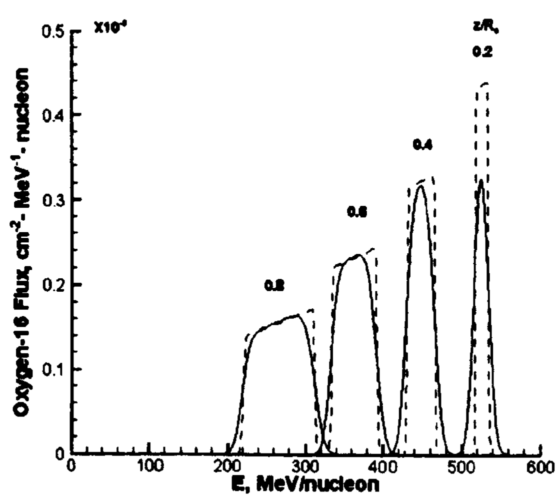

Fig. 6. First generation O(16,8) fragment flux at various depths compared with the same flux for the case in which the interaction energy width is zero (broken curve).

perturbative expansion of the solution (Wilson et al., 1991). The non-perturbative approximation lacks spectral details and assumes a broad near uniform distribution over the allowed energy domain (Wilson et al., 1991).

The effect of the collision energy downshift λ_{jk} is exhibited Figs. 4 and 5, where the flux of the first and second generation of $_8O^{16}$ ions is compared with the corresponding results for the case in which the downshift is zero. For the ions shown the shift is not great, contributing only a few MeV/nucleon. The downshift of more massive projectiles is somewhat larger.

Figs. 6 and 7 exhibit the effect of the interaction energy width ε_{jk} by comparing the flux of the first and second generation of $_8O^{16}$ ions with the corresponding results for the case in which the interaction energy width is zero. Significant widening occurs in the first generation of secondaries but little effect is seen in the second and presumably higher generations.

The effect of energy straggling on the the first and second generation of $_8O^{16}$ ions is exhibited Figs. 8 and 9, where the flux of of these ions is compared with the corresponding results for the case in which no energy straggling is present. In contrast with the results for the primary beam where straggling makes a significant contribution the effect on the first and second generation of secondaries appears to be relatively small.

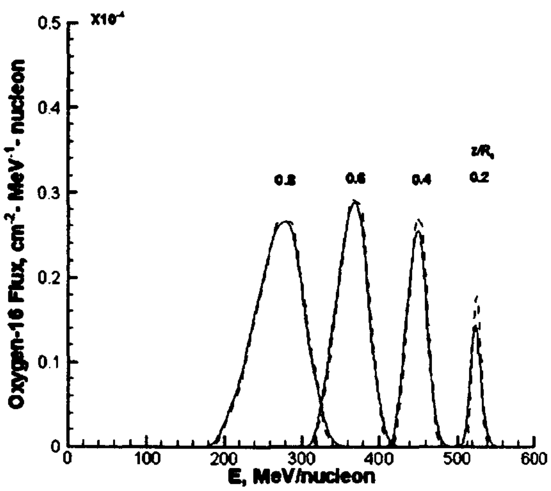

Fig. 7. Second generation O(16,8) fragment flux at various depths compared with the same flux for the case in which the interaction energy width is zero (broken curve).

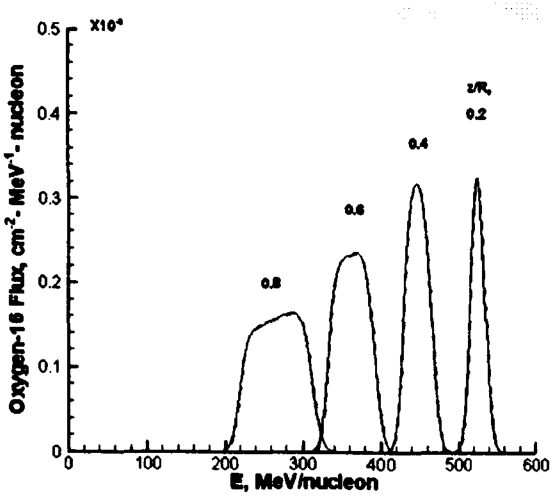

Fig. 8. First generation O(16,8) fragment flux at various depths compared with the same flux for the case in which there is no energy straggling (broken curve).

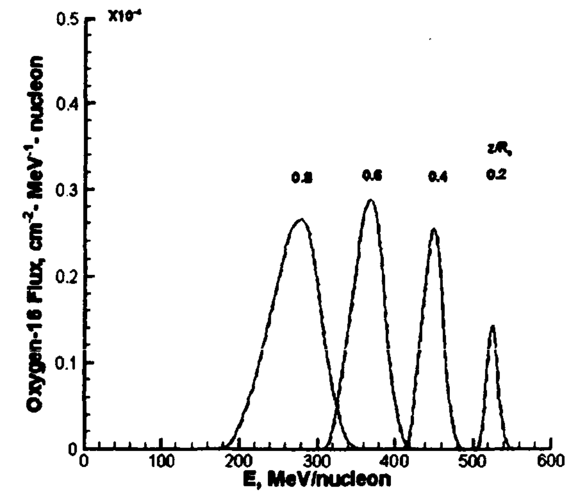

Fig. 9. Second generation O(16,8) fragment flux at various depths compared with the same flux for the case in which there is no energy straggling (broken curve).

5. Concluding remarks

The present formalism provides means of easy validation of material transmission properties in conventional laboratory setups at least to the third perturbation term. Higher order terms can be easily added using non-perturbation theory and assuming the third term spectral distribution. The next step is the simulation of the detector responses so that "raw" experimental data can be used to validate model predictions thereby simplyfying the validation process. Early versions of the Green's function code, when coupled with multiple elastic scattering in terms of acceptance functions (Shavers et al., 1993), showed great promise in describing HZE ion transport. In those studies, the straggling, energy downshift, and dispersion were neglected. The present formalism corrects those last remaining deficiencies. The recognition of the present formalism as the lowest order asymptotic term provides a systematic approach to more realistically treat a host of ion beam related problems. The next step will be to couple the multiple scattering propagator to the formalism and adding transverse momentum components to the first interaction term.

6. Uncited references

Schimmerling et al. (1999); Tschalar and Maccabee (1968).

References

Cucinotta, F.A., Wilson, J.W., Shinn, J.L., et al. Computational procedures and data base development, in: Wilson, J.W., Miller, J., Cucinotta, F.A. (Eds.), Shielding Strategies for Human Space Exploration, pp. 151–212, 1998.

Payne, M.G. Energy straggling of heavy charged particles in thick absorbers. Phys. Rev. 185 (2), 611–623, 1969.

Schimmerling, W., Rapkin, M., Wong, M., et al. The propagation of relativistic heavy ions in multi-element beam lines. Med. Phys. 13, 217–228, 1986.

Schimmerling, W., Wilson, J.W., Cucinotta, F.A., Kim, et al. Requirements for simulating space radiation with particle accelerators, in: Fujitaka, K., Majima, H., Ando, K., et al. (Eds.), Risk Evaluation of Cosmic-Ray Exposure in Long-Term Manned Space Mission. Kodansha Scientific Ltd, Tokyo, pp. 1–16, 1999.

Shavers, M.R., Frankel, K., Miller, J., Schimmerling, W., Townsend, L.W., Wilson, J.W. The fragmentation of 670 A MeV Neon-20 as a function of depth in water. III. Analytic multigeneration transport theory. Radiat. Res. 134 (1), 1–14, 1993.

Shinn, J.L., Wilson, J.W., Singleterry, R.C.etal Implications of microdosimetry in estimation of radiation quality in space environments. Health Phys. 76, 510–515, 1999.

Tripathi, R.P., Townsend, L.W., Khan, F. Role of intrinsic width in fragment momentum distributions in heavy ion collisions. Phys. Rev. C 48 (4), R1775–R1777, 1994.

Tschalar, C., Maccabee, H.D. Energy straggling measurements of heavy charged particles in thick absorbers. Phys. Rev. 165 (2), 2863–2869, 1968.

Wilson, J.W., Townsend, L.W., Schimmerling, W., et al. Transport Methods and Interactions for Space Radiations. NASA RP-1257, 1991.

Wilson, J.W. et al. Advances in space radiation shielding codes. J. Radiat. Res. 43 (Suppl.), S87–S91, 2002a.

Wilson, J.W., Tweed, J., Tai, H., et al. A simple model for straggling evaluation. Nucl. Instrum. Mater. B. 194, 389–392, 2002b (in press).